Indian Journal of Fibre & Textile Research
Vol. 51, September 2026, pp. 393-404
DOI: 10.56042/ijftr.v51i3.24186

Reinforcement of tapioca/glucomannan/poly(lactic acid) biothermoplastic composite using cellulose derivatives

B A Harsojuwono[1a], A Hartiati[1], N L Yulianti[2], R A Ilyas[3]

[1] Agricultural Industrial Technology Study Program, [2]Agricultural and Biosystems Engineering Study Program, Faculty of Agricultural Technology, Udayana University, Badung (80361), Bali, Indonesia

[3] Department of Chemical Engineering, Faculty of Chemical and Energy Engineering, Universiti Teknologi Malaysia

Received 25 September 2025; revised received and accepted 2June 2026

This research aims to determine the cellulose-derived filler that produces the best characteristics of the tapioca/glucomannan/polylactic acid (TP/GM/PLA) biothermoplastic composite. This research tried 10 treatments: control, use of microfibril cellulose (MFC), nanocrystalline cellulose (NCC), and nanofibril cellulose (NFC) with concentrations of 1.5, 2.5, and 3.5%, respectively. Measurements/observations: mechanical, physical, chemical, biodegradation, and thermal properties. The results showed that the TP/GM/PLA biothermoplastic composite with 2.5% NCC produced the best characteristics, with a tensile strength value of 24,668 MPa, elongation at break of 3.123%, Young's modulus of 1.843 GPA, and WVTR of 81.22 g/m^2.day, O_2TR of 85.46 ml/m^2.day, WHC of 0.17%, swelling of 2.92%, glass transition temperature of 60.98 ºC, crystallinity temperature of 68.19 ºC, melting point of 159.76 ºC, melt flow rate of 8.55 g/min, density of 1.25 g/cm^3, biodegradation time of 11.67 days. Furthermore, a 12% weight loss occurred up to 600 °C, with the highest DTA peak at 493.9°C with a value of 28 µV, and a crystallinity peak at a 2Θ angle of 29.51°C. This composite contains O-H (alcohol), C=O, C=C (aromatic ring), and C-O functional groups. The longitudinal surface profile contains small, densely packed spots with no obvious holes. The transverse surface profile shows all holes closed, compact, and dense.

Keyword: Biothermoplastic composite, Eco-friendly, Cellulose derivative, Tapioca, Glucomannan, Poly(lactic acid)

1 Introduction

Single-use plastics, made from petroleum, are a major cause of environmental pollution due to their difficulty in degrading[1,2]. In Indonesia, plastic pollution continues to increase, estimated to reach 23-27 million tons by 2040[3]. This is very concerning, necessitating the development of eco-friendly products, including alternatives to plastic cups. This idea is included in the government's goal number 2, specifically the green economy.

The development of eco-friendly plastic products requires semi-finished raw materials in the form of biothermoplastic composites. A potential and renewable natural-based semi-finished material for eco-friendly glass is the TP/GM/PLA biothermoplastic composite[4]. However, the ability of biothermoplastic composites to be made into eco-friendly molded products is greatly influenced by many factors, including the use of fillers[5].

The use of fillers aims to fill the pores of the composite to reduce water vapor and oxygen transmission and change the mechanical properties of the composite[6]. Douglas *et al.*:[7] explain that fillers such as cellulose, cellulose nanofibrils, and cellulose nanocrystals have been widely used to inhibit water vapor and oxygen transmission and improve the mechanical properties of composites. However, the ability to inhibit water vapor and oxygen transmission, suppress swelling, and change thermomechanical properties is highly dependent on the type and concentration of cellulose[8]. According to Douglas *et al.*:[7] and Aranda-Garcia *et al.*:[8], inappropriate use of cellulose and its derivatives will not be able to inhibit water vapor and oxygen transmission and change mechanical properties, even causing increased hardness, crystallinity, and melting temperature, making their application difficult.

Ilyas *et al.*:[9] reported that sisal fiber filler can increase the flexural modulus of thermoplastic starch/polylactic acid (TPS/PLA) composites. Filler of 1-5% micro/nanocrystalline cellulose increases thermal stability, relaxation temperature, and flexural properties of PLA by up to 40%[10]. Nanocellulose-reinforced TPS/PLA/PBS biothermoplastic composites have increased thermal, mechanical, and

[a] Corresponding author.
E-mail:bambang.admadi@unud.ac.id

oxygen resistance properties[11]. Biothermoplastic composites from a mixture of thermoplastic starch (TPS) and polylactic acid (PLA) experience a decrease in hygroscopicity as the content of bagasse fiber as a filler increases. Meanwhile, stress, strain, and flexural modulus increase as the content of bagasse fiber increases, but impact resistance decreases[8]. Smitthipong *et al.*:[12] reported that pineapple fiber-reinforced TPS/PLA mixtures are able to improve mechanostatic properties and water resistance. This also occurs when TPS/PLA is reinforced with cellulose derivatives[13]. TPS/PCL biothermoplastic composites reinforced with sisal fibers show increased tensile strength[14]. PLA biocomposites with 1-5% cellulose microfibers and nanocrystalline cellulose increase thermal stability, flexural mechanical properties by up to 40%, and storage modulus by approximately 35% at room temperature. Furthermore, the addition of nanocrystalline cellulose increases the material's relaxation temperature from 50 to 60°C, thus expanding its temperature range[15]. The tensile strength and hydrophobicity of TPS/PLA composites increase with increasing ramie fiber content, ranging from 1-25% of the matrix weight[16].

This description indicates that there is little information on the use of cellulose-derived fillers in reinforcing TP/GM/PLA biothermoplastic composites. Therefore, the use of cellulose derivatives in reinforcing TP/GMPLA biothermoplastic composites needs to be studied. The aim of this study was to determine the cellulose derivative that produces the best characteristics of the TP/GM/PLA biothermoplastic composite.

2 Materials and Methods

2.1 Materials

Materials: tapioca and glucomannan (CV Nurajaya), glycerol and distilled water (CV Brathacem), anhydrous maleic acid (AMA), polylactic acid (PLA) (CV Bandung), microfibrillar cellulose (MFC), nanofibrillar cellulose (NFC), nanocrystalline cellulose (NCC) (CV Sukses Makmur).

Tools: screw extruder (Model: TDD20, Prod: USEON Tech), rheomix 3000 (Type: PTW1625, Prod: Rheology Solutions PTY LTD), hydraulic hot press (Type: TMAX-SYP-3T, Prod: Tmax company), mixer (Type: DMX-B7C, Prod: FOMAC), grinder (Type: HR1500, Prod: FOMAC), WVTR Tester (type: W203H, 3 test chambers), O_2TR Tester brand: Maxtec, A+R217), Thermal Gravimetry Analyzer (brand: Bonnin Tech, type: TGA 101), X-ray Diffractometer (Brand: MAXima, goniometer=PW3050/60 (Theta/Theta), Scanning Electron Microscopy (Low vacuum electron microscope, type: JSM - IT 200, brand: JEOL), FTIR Spectrometer (Brand: Shimadzu IR Prestige - 21, type: 206-73600-36, series: A21005002919).

2.2 Methods

2.2.1 Research Stages

Research stages: 1) preparation: production of thermoplastic tapioca (TT) and thermoplastic glucomannan (GT), 2) main research: determination of cellulose-derived fillers in the production of TP/GM/PLA biothermoplastic composites. The description is as follows.

2.2.1.1 Preparation: Production of TT and GT

The materials for the production of TT were weighed: 100 kg of tapioca, 25 kg of glycerol, and 15 kg of distilled water. The materials for the production of GT were weighed: 33 kg of glucomannan, 8.3 kg of glycerol, and 5 kg of distilled water. Separately, for the production of TT and GT, glycerol and distilled water were mixed and stirred until homogeneous. Then, tapioca or glucomannan was added gradually until the mixture was used up while stirring (240 rpm, 10 minutes). The homogenous dough was aged for 8 days at room temperature, then rheomixed (50 rpm, 90 ^{o}C, 15 minutes), resulting in TT and GT lumps. Both were floured and sieved to a size of 90-100 mesh to produce TT and GT flour[17,18].

2.2.1.2 Main research: Determination of cellulose derivatives in the manufacture of TP/GM/PLA biothermoplastic composites.

This study used a randomized block design with a control treatment, using MFC, NFC, and NCC, each with filler concentrations of 1.5%, 2.5%, and 3.5%, resulting in 10 treatments across three processing time groups, resulting in 30 experimental units.

2.2.1.3 Procedure

The procedure was as follows: weigh 1 kg of TT (1 kg); 0.33 kg of GT (0.33 kg); 2.45 kg of PLA; 0.3 kg of AMA; and add filler according to the treatment: control, using MFC, NFC, using NCC with concentrations of 1.5%, 2.5%, and 3.5%, respectively. All powdered ingredients were mixed and stirred (240 rpm for 1 minute), then fed into a hot screw pellet machine (110°C, 50 rpm). The resulting pellets were pressed using a hot press at 130°C and 50 bar for

5 mins to form a 0.02 mm thick TP/GM/PLA thermoplastic biocomposite sheet (modification[19]).

The sheets were then tested for quality variables including tensile strength, elongation at break, and Young's modulus (following ASTM D638 procedure), swelling (following ASTM D570), water vapor transfer rate (WVTR) and water holding capacity (WHC) (following ASTM E96/E96M-21, oxygen transfer (O_2TR) (following ASTM D3985-17), glass transition temperature (Tg), crystallinity temperature (Tc) and melting point (MP) (following ASTM D3418), melting flow rate (MFR) (following D1238), biodegradation time (ISO 846:2019), density (following ASTM D792-20 procedure), thermal stability (using thermal gravimetric analyzer/TGA, sample size: 20 mg, dry N_2 flow rate: 140 mL/min, operating temperature: 25-500 °C, temperature flow rate: 10 °C/min, pressure: 1 atm), crystallinity (using X-ray diffractometer/XRD, brand: MAXima type XRD-7000, diffractometer type: 0000000011063758, sample: powder, sample size: 1 mg, anode material: Cu, CuK α radiation (λ=1.54 Å), relative intensity at 2Θ: 10-80°, K-A2/K-A1 ratio: 0.500, goniometer radius: 240 mm, measurement temperature: 25 °C, voltage: 40 kV, electric current: 40 mA), surface profile (using Scanning Electron Microscope/SEM, low vacuum electron microscope, type: JSM - IT 200, brand: JEOL, sample: solid, sample size: 1 cm x 1 cm, filament voltage: 1.5 KV, sensor: sondary electron detector) and functional group profile (using FTIR spectrometer, Brand: Shimadzu IR Prestige-21, type: 206-73600-36, series: A21005002919, sample shape: solid, sample size: small piece 0.5 cm x 0.5 cm, measurement mode: % transmittance, anodization: happ-genzel, resolution: 2.0 cm^{-1}, wavenumber range: 340-4700 cm^{-1}, beam: internal, detector: standard, mirror speed: 2.8 TP, IFG noise: 1, IFG similarity: 1, IR range: medium)[4,5,17].

2.2.2 Data analysis

The measurement data were analyzed of variance and then followed by HSD Tukey's difference test using SPSS 25.0. Graphical data were analyzed descriptively, qualitatively, and quantitatively. The determination of the best treatment was based on the most abundant quality variables in accordance with SNI 1778:2014.

3 Results and Discussion

3.1 Tensile Strength, Elongation at Break, and Young's Modulus

Analysis of Variance showed that cellulose derivatives significantly affected the tensile strength, elongation at break, and Young's modulus of the TP/GM/PLA biothermoplastic composite. The average tensile strength ranged from 18.113 to 24.668 MPa, elongation at break from 3.123 to 7.171%, and Young's modulus from 1.425 to 1.843 GPa, as shown in Table 1.

The highest tensile strength (24.668 MPa) was found in the TP/GM/PLA biothermoplastic composite using 2.5% NCC, significantly different from the others. Meanwhile, the lowest tensile strength (18.113 MPa) was found in the control composite and significantly different from the others.

The highest elongation at break (7.171%) was found in the control, which was not significantly different from the elongation at break of the biothermoplastic composite using 1.5-2.5% MCC. Meanwhile, the lowest elongation at break (3.123%) was found in the TP/GM/PLA biothermoplastic composite using 2.5% NCC, which was not significantly different from the TP/GM/PLA biothermoplastic composites using 1.5% and 3.5% NCC.

The highest Young's modulus (1.843 GPa) was found in the TP/GM/PLA biothermoplastic composite using 2.5% NCC, which was significantly different from the other composites. Meanwhile, the lowest Young's modulus (1.425 GPa) was found in the control, which was significantly different from the other composites.

These results support the opinion of Kargarzadeh *et al.*:[20], who explained that, in general, nanocellulose-reinforced PLA biocomposites contribute to increased tensile strength and elastic modulus. Ilyas *et al.*:[21] explained that the use of NCC as a reinforcement for starch-based polymers

Table 1 — Mean of tensile strength, elongation at break, and Young's modulus of TP/GM/PLA biothermoplastic composites in various cellulose derivatives

Treatment	Mean of tensile strength (MPa)	Mean of elongation at break (%)	Mean of Young's modulus (GPa)
Control	18.113f	7.171a	1.425e
MCC 1.5%	20.104e	6.982ab	1.635d
MCC 2.5%	20.815e	6.193ab	1.653cd
MCC 3.5%	20.944e	6.124bc	1.668cd
NCC 1.5%	23.346b	3.372ef	1.766b
NCC 2.5%	24.668a	3.123f	1.843a
NCC 3.5%	23.165bc	3.434ef	1.771b
NFC 1.5%	22.634cd	5.562cd	1.737bc
NFC 2.5%	22.463cd	5.132cd	1.694bc
NFC 3.5%	22.114d	4.961de	1.642cd

Note: The same notation after the average in the same column indicates no significant difference at the 5% error level

produces the right conditions because NCC contains many hydroxyl groups. The hydroxyl groups on the NCC surface are responsible for the formation of hydrogen bonds between the non-polar matrix and the –OH groups of the hydrophilic polymer matrix. In addition, the proper use of NCC will increase the mechanical strength of the new material and also facilitate biodegradation[22].

The use of MCC and NCC as fillers tends to increase the stiffness and strength of the composite, thereby reducing elongation at break. However, this can be influenced by other factors such as dispersion, polymer-particle interface, and polymer matrix type[23]. Meanwhile, Simangungsong *et al.*:[24] explained that the addition of NCC as a filler in PLA composites increased the elongation at break, with the highest percentage reaching 19.02% for a 1% NCC filler addition. However, higher additions actually decreased the elongation at break.

The tensile strength and Young's modulus between nanocellulose and the biopolymer matrix play a crucial role in the biocomposite interface, achieving efficient load transfer from the matrix to the nanocellulose[25]. According to Zhang *et al.*:[26], Young's modulus increased with increasing NCC loading up to 15% due to the good dispersion of NCC in the PLA matrix. Meanwhile, the use of low MCC (1%) increased polymer chain mobility and contributed to higher matrix chain elasticity, as well as higher tensile strength (1.2%) and higher elastic modulus (12.1%)[27].

Ilyas *et al.*:[21] reported that the addition of 0.5% by weight of sugar palm nanocellulose was able to increase the tensile strength and Young's modulus of the composite, by 11.47 and 178.83 MPa, respectively. Furthermore, it was explained that the Young's modulus of the nanocomposite film was six times higher than the Young's modulus of the film from starch reinforced with sugar palm cellulose microfibrils. Meanwhile, Kaya *et al.*:[23] explained that the effect of NCC was greater than MCC on tensile strength and Young's modulus because the size of NCC was smaller and its crystallinity was higher. The increase in SNCC in PLA-based composite films caused an increase in mechanical properties compared to the control. PLA composites with 0.5 wt% SNCC showed an increase in tensile strength and elongation at break by 53.87% and 61.46%, respectively[28]. The addition of 1 wt% NCC to pure PLA increased the tensile strength by 19.04% (from 48.41 to 57.63 MPa) and the elastic modulus by 13.47% (from 1791.62 to 2033.07 MPa)[29]. NCC improved the mechanical properties of the composites by increasing stiffness and improving interfacial bonding[30,31].

3.2 WVTR, O2TR, WHC, and Swelling

Analysis of variance showed that cellulose derivatives significantly affected the WVTR, O_2TR, WHC, and swelling of the TP/GM/PLA biothermoplastic composite. The average WVTR values ranged from 81.22 to 118.76 g/m²/day, O_2TR from 85.46 to 129.66 ml/m²/day, WHC from 0.17 to 0.911%, and swelling from 2.92 to 8.12%, as shown in Table 2.

The highest WVTR value (118.76 g/m²/day) was found in the TP/GM/PLA biothermoplastic composite without filler (control), significantly different from the others. Meanwhile, the lowest WVTR value (81.22 g/m^2.day) was found for the TP/GM/PLA biothermoplastic composite using 2.5% NCC, which was not significantly different from the WVTR of the composite using 3.5% NCC.

The highest O_2TR value (129.66 ml/m^2.day) was found for the control, significantly different from the other composites. Meanwhile, the lowest O_2TR value (85.46 ml/m^2.day) was found for the TP/GM/PLA biothermoplastic composite using 2.5% NCC, which was not significantly different from the O_2TR of the composite using 3.5% NCC.

The highest WHC value (0.91%) was found for the control, significantly different from the other composites. Meanwhile, the lowest WHC value (0.17%) was found for the TP/GM/PLA biothermoplastic composite using 2.5% NCC, which was not significantly different from the WHC of the composite using 3.5% NCC.

The highest swelling value (8.12%) was found in the control, significantly different from the others.

Table 2 — Average WVTR, O2TR, WHC, and swelling of TP/GM/PLA biothermoplastic composites in various cellulose derivatives

Treatment	Mean of WVTR (g/m^2.hari)	Mean O_2TR (ml/m^2.hari)	Mean of WHC (%)	Mean of swelling (%)
Control	118.76a	129.66a	0.91a	8.12a
MCC 1.5%	90.89b	94.97b	0.31b	4.92b
MCC 2.5%	89.32b	92.65b	0.29b	4.67b
MCC 3.5%	84.34cd	90.45bc	0.26bc	4.19bc
NCC 1.5%	85,78cd	87.98cd	0.19cd	3.10cd
NCC 2.5%	81.22e	85.46e	0.17e	2.92e
NCC 3.5%	82.55de	85.93de	0.18de	3.05de
NFC 1.5%	88.90bc	90.77b	0.20cd	3.28cd
NFC 2.5%	86.67bc	87.22cd	0.19de	3.20cd
NFC 3.5%	83.87cd	86.45de	0.18de	3.11cd

Note: The same notation after the average in the same column indicates no significant difference at the 5% error level

Meanwhile, the lowest swelling value (2.92%) was found in the TP/GM/PLA biothermoplastic composite using 2.5% NCC, which was not significantly different from the swelling of the composite using 3.5% NCC.

Ilyas *et al.*:.[32] explained that NCC has been shown to reduce the water vapor permeability of starch-based films by increasing the film's tortuosity. The high compatibility of the starch matrix and nanocellulose fillers increases the film's sensitivity to water, making it suitable for food packaging applications. The inclusion of nanocellulose, both NCC and NFC, into chitosan, reduces the water vapor permeability of the composite film because water vapor diffuses more easily through the amorphous region with a low crystallinity index[25,33]. Othman *et al.*:.[34] explained that the water absorption capacity of chitin and chitosan increases with decreasing crystallinity index. Trifol *et al.*:[33] explained that pure PLA reinforced with nanocellulose, either NCC or NFC, resulted in a decrease in the oxygen transmission rate (O_2TR) of up to 90% and the water vapor transmission rate (WVTR) of up to 76% of the hybrid nanocomposite film. The increase in SNCC in PLA-based composite films was proven to provide an increase in air permeability compared to the control[28].

3.3 Glass Transition Temperature, Crystallinity Temperature, Melting Point, and Melt Flow Rate

Analysis of variance showed that cellulose derivatives significantly affected the glass transition temperature, crystallinity, melting point, and melt flow rate of the TP/GM/PLA biothermoplastic composite. The average glass transition temperature ranged from 54.78 to 60.98°C, the crystallinity temperature from 61.18 to 68.19°C, the melting point from 1152.94 to 159.67°C, and the melt flow rate from 8.23 to 12.17 g/min, as shown in Table 3.

The highest glass transition temperature (60.98°C) was found in the TP/GM/PLA biothermoplastic composite containing 2.5% NCC, which was not significantly different from the glass transition temperature of the biothermoplastic composite containing 3.5% NCC. Meanwhile, the lowest glass transition temperature (54.78°C) was achieved by the control, which was not significantly different from the glass transition temperature of the TP/GM/PLA biothermoplastic composite using 1.5% MCC.

The highest crystallinity temperature (68.19°C) was achieved by the TP/GM/PLA biothermoplastic composite using 2.5% NCC, which was not significantly different from the crystallinity temperature of the biothermoplastic composite using 3.5% NCC. Meanwhile, the lowest crystallinity temperature (61.18°C) was achieved by the control, which was not significantly different from the crystallinity temperature of the TP/GM/PLA biothermoplastic composite using 1.5% MCC.

Table 3 — Mean of glass transition temperature, crystallinity temperature, melting point and melt flow rate of TP/GM/PLA biothermoplastic composites in various cellulose derivatives

Treatment	Mean of glass transition temperature (°C)	Mean of crystallinity temperature (°C)	Mean of melting point (°C)	Mean of melt flow rate (g/min)
Control	54.78f	61.18f	152.94f	12.17a
MCC 1.5%	55.34ef	63.23ef	154.74ef	11.64ab
MCC 2.5%	57.98de	65.55de	155.34de	10.60bc
MCC 3.5%	58.23cd	66.38cd	156.45cd	9.95cd
NCC 1.5%	59.98bc	67.42bc	157.12bc	9.59cd
NCC 2.5%	60.98a	68.19a	159.76a	8.23f
NCC 3.5%	60.08ab	67.99ab	158.98ab	8.65ef
NFC 1.5%	58.33cd	66.84cd	157.06bc	9.46cd
NFC 2.5%	59.12bc	67.24bc	158.67ab	9.19de
NFC 3.5%	60.04ab	67.31bc	158.76ab	8.93de

Note: The same notation after the average in the same column indicates no significant difference at the 5% error level

The highest melting point (159.76°C) was achieved by the TP/GM/PLA biothermoplastic composite using 2.5% NCC, which was not significantly different from the melting point of the TP/GM/PLA biothermoplastic composite using 3.5% NCC. Meanwhile, the lowest melting point (152.94°C) was found in the control, which was not significantly different from the melting point of the TP/GM/PLA biothermoplastic composite using 1.5% MCC.

The highest melt flow rate (12.17 g/min) was found in the control, which was not significantly different from the melt flow rate of the TP/GM/PLA biothermoplastic composite using 1.5% MCC. Meanwhile, the lowest melt flow rate (8.23 g/min) was found in the TP/GM/PLA biothermoplastic composite using 2.5% NCC, which was not significantly different from the melt flow rate of the TP/GM/PLA biothermoplastic composite using 3.5% NCC.

The compatibility between NCC and polymer matrix is an important factor that determines the thermal properties of polymer composites. The presence of NCC or MCC limits the movement of polymer chains, especially in the amorphous region[23]. Tomec *et al.*:[27] explained that polymer movement requires greater energy which causes an increase in

the glass transition temperature. This increase in the glass transition is often associated with an increase in crystallinity. Increasing the nanofiller content in the polymer matrix causes an increase in crystallinity which causes an increase in a more ordered structure, so that the transition to a glass requires a higher temperature[35]. However, the addition of nanofillers such as NCC, NFC that are not appropriate can disrupt the existing crystal structure of the polymer matrix, which has an impact on reducing its melting temperature[27]. Gan *et al.*:[35] explained that the interaction of NCC with the polymer can affect the viscosity of the composite melt. Strong interactions between micro- and nanocellulose and composite polymers can increase viscosity and decrease melt flow rates. Conversely, weak interactions can result in lower melt flow rates[36]. Tomec *et al.*:[27] explained that the use of low MCC (1%) increases polymer chain mobility and contributes to matrix chain elasticity and higher crystallinity, a lower glass transition temperature (1.66 °C), and a lower melting temperature (1.31 °C).

Zhang *et al.*:[26] showed that NCC loading enhances the film's liquid-to-solid transition at high temperatures. Furthermore, the onset temperature of thermal decomposition also increases with the addition of NCC[23]. Tomec *et al.*:[27] explained that the crystallization temperature increases with the addition of micro- and nanocellulose as nucleating agents, which impacts polymer chain kinetics[23,27].

Khoo *et al.*:[37] showed that increasing NCC leads to an increase in decomposition temperature and accelerates crystallization. PLA with 5% NCC produced higher crystallinity (34.5%) compared to pure PLA (30.9%). Kusmono and Wiratma[29] explained that the PLA/NCC composite exhibited two weak endothermic peaks at temperatures around 65 and 166°C and a sharp endothermic peak at around 353°C. The weak endothermic peak at around 65°C indicates the glass transition temperature, while the weak endothermic peak at around 166°C indicates the melting point of pure PLA. The sharp endothermic peak at around 350°C indicates the decomposition or degradation of the pure PLA chains[38].

Bazan *et al.*:[39] explained that the thermal characteristics of PLA/PHBV composites using NCC exhibited an exothermic peak in the range of 85–120°C, which is the post-crystallization temperature [40,41]. The endothermic peak occurred at 140–180°C, which is the melting temperature of the crystallites [42,43]. Meanwhile, the glass transition temperature (Tg) occurs at 55°C which indicates the thermal stability of the composite[44]. NCC increases nucleation activity, facilitates crystallization, and improves thermal stability through interaction with the polymer matrix [45,46].

3.4 Density and Biodegradation Time

Analysis of variance showed that cellulose derivatives significantly affected density but not biodegradation time of TP/GM/PLA biothermoplastic composites. The average density ranged from 1.23 to 1.29 g/cm^3, while the average biodegradation time ranged from 11.67 to 12.33 days, as shown in Table 4.

The TP/GM/PLA biothermoplastic composites containing 2.5 to 3.5% MCC exhibited high densities (1.28 to 1.29 g/cm^3), which were not significantly different from those of the TP/GM/PLA biothermoplastic composites containing 1.5% MCC. Meanwhile, the control composites had the lowest density (1.23 g/cm^3), which was not significantly different from the densities of the TP/GM/PLA biothermoplastic composites containing 1.5% NCC and NFC.

The above density shows similar results from the study by Bazan *et al.*:[39], which showed that PLA/PHBV composites with NCC ranged from 1.24 to 1.27 g/cm^3. According to Omran *et al.*:[36], NCC has a relatively high intrinsic density compared to many polymer matrices, namely 1.49 g/cm^3 [39]. When combined with PLA, NCC will fill the empty spaces or pores, especially in the amorphous part, thereby reducing porosity and increasing the polymer density, thus increasing the overall density[24]. The addition of nanocellulose, which replaces part of the composite

Table 4 — Average density and biodegradation time of TP/GM/PLA biothermoplastic composites in various cellulose derivatives

Treatment	Mean of density (g/cm^3)	Mean of biodegradation time (day)
Control	1.23e	11.67a
MCC 1.5%	1.27ab	12.00a
MCC 2.5%	1.28a	12.33a
MCC 3.5%	1.29a	11.67a
NCC 1.5%	1.24de	12.00a
NCC 2.5%	1.25cd	11.67a
NCC 3.5%	1.26bc	12.00a
NFC 1.5%	1.24de	12.33a
NFC 2.5%	1.25cd	11.67a
NFC 3.5%	1.26bc	11.67a

Note: The same notation after the average in the same column indicates no significant difference at the 5% error level

volume, causes an increase in mass, which impacts the increase in density[47].

The biodegradation time value of the TP/GM/PLA biothermoplastic composite showed no significant difference for all treatments. This indicates that the composite can decompose well around the 12th day. This is in accordance with the opinion of Xu *et al.*:[48], who reported that biocomposite biodegradation ranges from 7 to 45 days. Meanwhile, according to SNI 1778:2014, the maximum biodegradation time for biodegradable products is 60 days. Essentially, the biodegradability of a material results from natural degradation by microorganisms (composting) and subsequent mineralization into carbon dioxide (CO_2) and/or methane (CH_4), H_2O, and inorganic salts.

3.5 Thermal Stability

The relationship between temperature and weight of the TP/GM/PLA biothermoplastic composite during the heating process is shown in Fig. 1 As the temperature increases, the weight percentage decreases. Weight loss for the control composite begins at 306.1°C, while for the TP/GM/PLA biothermoplastic composites using MCC, NCC, and NFC, weight loss begins at 312.3, 359.9, and 345.6°C, respectively. Weight loss becomes more pronounced at temperatures ranging from 358.7 to 409.7°C for the control composite, 363.5 to 407.3°C for the MCC composite, 376.7 to 408.8°C for the NCC composite, and 369.2 to 411.4°C for the NFC composite. Subsequently, all composites experience a more horizontal weight loss at a relatively similar angle up to 600°C[49].

Fig. 1 also shows that the TP/GM/PLA biothermoplastic composite using NCC has lower weight loss than the others. This is in accordance with the opinion of Zhang *et al.*:.[26] who showed that NCC loading increases the transition from liquid to solid at high temperatures. It is further explained that the dispersion of NCC in the PLA matrix up to 15% still occurs very well. Fig. 1 also shows that the TP/GM/PLA biothermoplastic composite with NCC has better thermal stability than the others. This result is in accordance with the opinion of Raghu *et al.*:.[50] who explained that NCC has a high crystalline structure and the ability to form strong hydrogen bonds, which causes an increase in the thermal stability of the TPS/PLA composite. Thus inhibiting the thermal degradation of nanocellulose-reinforced composites[35].

The relationship between temperature and differential thermal analysis (DTA) of the TP/GM/PLA biothermoplastic composite during the heating process can be seen in Fig. 2. Increasing the temperature to 129.8°C for the control, 133.2°C for the composite with MCC, 137.9°C for the composite with NCC, and 134.5°C for the composite with NFC resulted in a decrease in DTA of -7.89, -8.780, -9.47, and -9.09 µV, respectively. Furthermore, increasing the temperature to 373°C for the control, 378.1°C for the composite with MCC, 372.5°C for the composite with NCC, and 399.2°C for the composite with NFC resulted in a very high increase in DTA. Furthermore, there was a decrease in DTA up to a temperature of 388.1°C for the control, 389.7°C for the composite

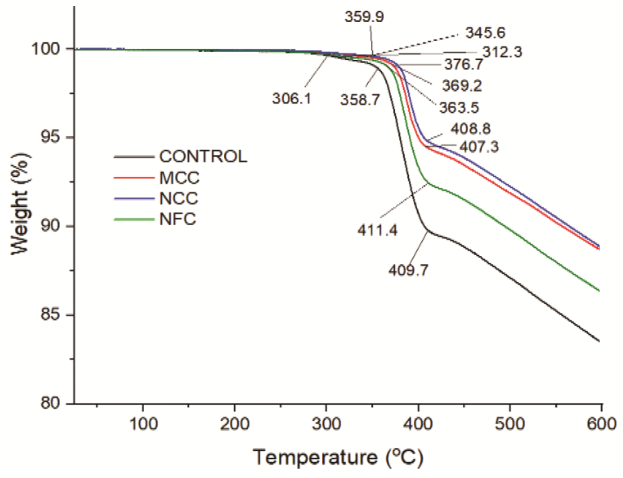

Fig. 1 — Relationship between temperature and weight of TP/GM/PLA biothermoplastic composites in various cellulose derivatives during heating

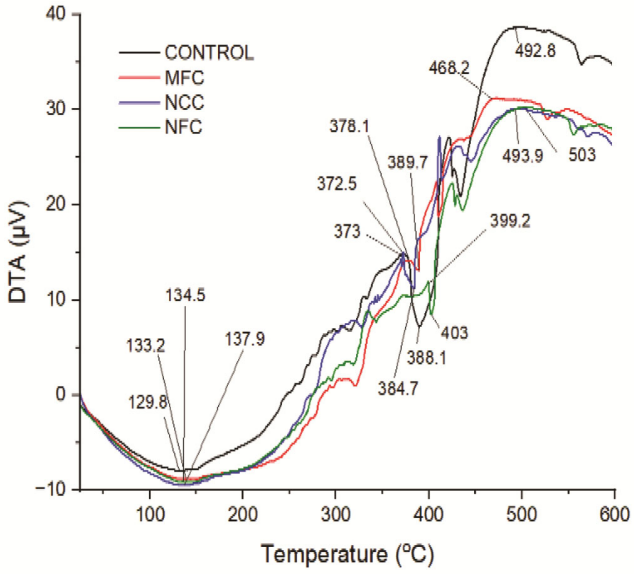

Fig. 2 — Relationship between temperature and differential thermal analysis (DTA) of the TP/GM/PLA biothermoplastic composite in varying cellulose derivatives during heating

with MCC, 384.7°C for the composite with NCC, 403°C for the composite with NFC. The subsequent increase in temperature increased the DTA up to a temperature of 492.8°C for the control, 468.2°C for the composite with MCC, 493.9°C for the composite with NCC, 503°C for the composite with NFC. Furthermore, there was a decrease in DTA up to a temperature of 600°C.

According to Raghu *et al.*:[50], a decrease in DTA means that heat is released due to a phase transition or chemical reaction in the composite. It is further explained that an increase in DTA causes the absorption of heat from outside by the composite which can change the polymer structure. However, TP/GM/PLA biothermoplastic composites with different fillers experience a decrease or increase in DTA at different temperatures. This is due to differences in cellulose derivatives and the interaction ability between the filler and the polymer matrix 16. According to Ilyas *et al.*: [51], the polymer decomposition temperature increases with increasing NCC loading. This indicates that NCC increases thermal stability and slows down the rate of thermal degradation[35] Kusmono and Wiratma[29] explained that the PLA/NCC composite showed a sharp endothermic peak at a temperature of around 353°C. The sharp endothermic peak at a temperature of around 350°C indicates the decomposition or degradation of pure PLA chains[49].

3.6 Crystallinity

The relationship between the 2Θ angle and the diffraction intensity of the TP/GM/PLA biothermoplastic composite can be seen in Fig. 3. Fig. 3 shows that the highest diffraction intensity was achieved at an angle of 2Θ = 29.37° for the control, an angle of 2Θ = 29.41° for the TP/GM/PLA biothermoplastic composite with MCC, an angle of 2Θ = 29.51° for the composite with NCC, and an angle of 2Θ = 29.33° for the composite with NFC. In addition, there are several other peaks at angles of 2Θ = 23.03° and 30.87° for the control, 23.09 and 30.97° for the composite with MCC, 23.19 and 31.03° for the composite with NCC, and 22.95 and 30.79° for the composite with NFC.

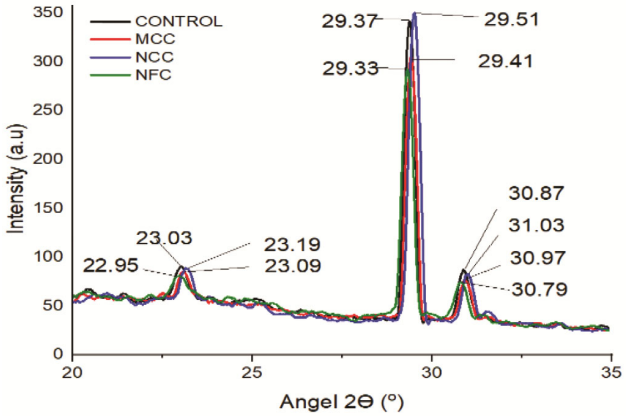

Fig. 3 — Relationship between the 2Θ angle and diffraction intensity of the TP/GM/PLA biothermoplastic composite in various cellulose derivatives

Fig. 3 shows that the use of NCC in the production of the TP/GM/PLA biothermoplastic composite significantly increased crystallinity, as indicated by a peak area at the 2Θ angle of 29.33° compared to the other cellulose derivatives. This is in line with Ilyas *et al.*:[51], who explained that NCC enhances PLA crystallization, as evidenced by PLA/NCC-5 exhibiting higher crystallinity (34.5%) compared to pure PLA (30.9%).

Increasing the amount of nanocellulose, including NCC and NFC, further increased the degree of crystallinity due to crystallization[47,48]. In general, NCC acting as a nucleating agent will increase the crystallinity of the polymer matrix, thereby increasing crystallization and brittle properties[35]. The addition of 2% NCC to the PLA composite resulted in higher crystallinity (37.8%) compared to other nanocomposites[52]. This is due to improved alignment and packing of NCC within the polymer matrix, thereby increasing the crystallinity of the nanocomposite. This is evidenced in the crystallization of the PLLA/PEG/NCC nanocomposite[53].

3.7 Functional Group Profile

Fig. 4 and Table 5 show the wavenumbers and functional groups of the control and the biothermoplastic TP/GM/PLA composites with MCC, NCC, and NFC. The control has an O-H

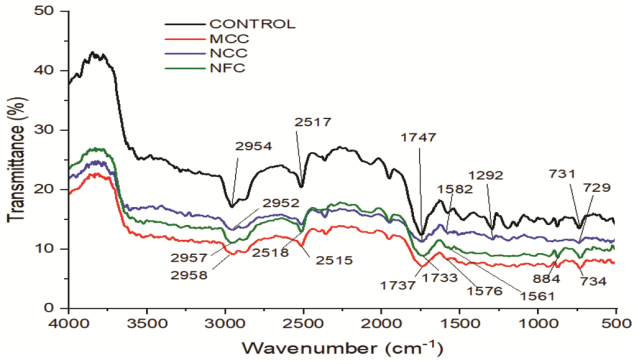

Fig. 4 — Wavenumber and functional groups of TP/GM/PLA biothermoplastic composite

Table 5 — Wavenumbers and functional groups of TP/GM/PLA biothermoplastic composites as a control and using MCC, NCC, and NFC

Standard wavenumber area (cm^{-1})	Standard functional groups	Control	+MCC	+NCC	+NFC
2000-3600	O-H alcohol	O-H alcohol	O-H alcohol	O-H alcohol	O-H alcohol
1690-1760	C=O	C=O	C=O	C=O	C=O
1500-1600	C=C (aromatic ring)	C=H	C=C (aromaticring)	C=C (aromaticring)	C=C (aromaticring)
900-1300	C-O		C=H	C-O	C=H
650-1000	C=H			C=H	

(alcohol) functional group at wavenumbers 2954 and 2517 cm^{-1}, C=O at wavenumber 1747 cm^{-1}, and C=H at wavenumber 731 cm^{-1}.

The biothermoplastic TP/GM/PLA composite with MCC has an O-H (alcohol) functional group at wavenumbers 2958 and 2515 cm^{-1}, C=O at wavenumber 1737 cm^{-1}, C=C (aromatic ring) at wavenumber 1576 cm^{-1}, and C=H at wavenumber 734 cm^{-1}.

The TP/GM/PLA biothermoplastic composite with NCC has an O-H (alcohol) functional group at wavenumber 2952 cm^{-1}, C=O at wavenumber 1747 cm^{-1}, C=C (aromatic ring) at wavenumber 1582 cm^{-1}, C-O at wavenumber 1292 cm^{-1}, and C=H at wavenumber 729 cm^{-1}.

The TP/GM/PLA biothermoplastic composite with NFC has an O-H (alcohol) functional group at wavenumbers 2957 and 2518 cm^{-1}, C=O at wavenumber 1733 cm^{-1}, C=C (aromatic ring) at wavenumber 1561 cm^{-1}, and C=H at wavenumber 884 cm^{-1}.

According to Ilyas *et al.*:.[51], the addition of NCC to starch- and PLA-based composites causes interactions between hydroxyl groups (from starch) and NCC through hydrogen bonding or other reactions, which alter the functional group environment within the composite, such as the appearance of C-O groups at a wavenumber of 1292 cm^{-1}. This indicates that the functional group content of the TP/GM/PLA biothermoplastic composite with NCC differs from that of other composites. Meanwhile, Muller *et al.*:[54], explained that peaks characterized by C-O stretching vibrations indicate the presence of amylose and amylopectin.

Tsioptsias *et al.*:.[55] reported that C=O vibrations occur at wavenumbers 1,780–1,713 cm^{-1} in the compatibilizer spectrum, caused by symmetric C=O stretching in the anhydride and carboxylic acid groups. Furthermore, Nazrin *et al.*:[56], showed that the O-H functional group experiences a small wavenumber shift, indicating strong inter- and intramolecular hydrogen bonds in the starch chain. This reflects that mixing PLA with starch increases the hydrogen bonding of starch molecules.

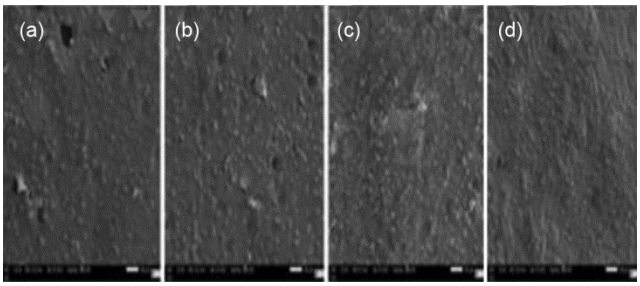

Fig. 5 — Longitudinal surface profiles of TP/GM/PLA biothermoplastic composites using (a) Control, (b) MCC, (c) NCC, (d) NFC

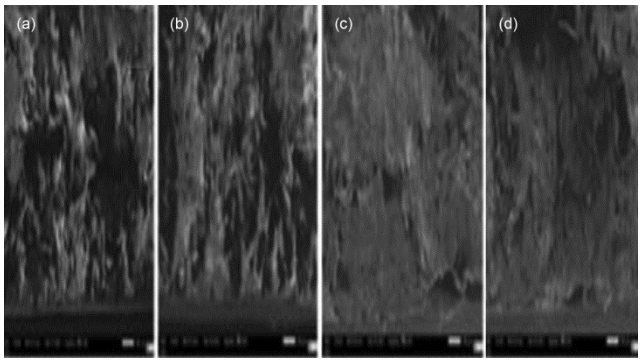

Fig. 6 — Transverse surface profile of TP/GM/PLA biothermoplastic composites using (a) control, (b) MCC, (c) NCC, (d) NFC

3.8 Surface Profile

Fig. 5 displays the longitudinal surface profiles of the control and TP/GM/PLA biothermoplastic composites using MFC, NCC, and NFC. Fig. 5 shows a clear difference in surface profiles. The control surface profile shows relatively large, rough spots and relatively deep voids. Meanwhile, the TP/GM/PLA composite using MFC still shows relatively large, rough spots and some shallow voids. The composite using NCC still has spots, but they are smaller and more closely spaced, with no obvious voids. The composite using NFC shows slightly larger, more evenly distributed spots than the NCC composite, and is smoother, but still contains some indistinct voids.

Fig. 6 displays the transverse surface profiles of the control and TP/GM/PLA biothermoplastic composites using MFC, NCC, and NFC. The differences in

appearance are clear. The control surface profile shows large, deep voids and an irregular, rough appearance. Meanwhile, the composite using MFC still exhibited holes, but they were narrower, less deep, and coarser. The composite using NCC showed almost all the holes closed and was more compact and dense. The composite using NFC showed closed, layered holes and was quite compact and dense. Furthermore, regular fibers were also visible.

The use of fillers such as MCC, NCC, and NFC tends to increase the surface roughness of PLA composites compared to pure PLA[9,11,21,34]. This is consistent with Ilyas *et al.*:[32], who explained that pure palm sugar starch films have smoother surfaces than palm sugar starch films containing NCC. However, Bazan *et al.*:[39] explained that PLA/PHBV composites with NCC have smoother surfaces compared to other cellulose fillers, exhibiting very rough, complex, and irregular structures. This is due to increased intercomponent bonding with the hydrophilic filler and the interaction of hydroxyl groups with the polymer matrix[10]. However, the use of appropriate compatibilizers can improve the compactness and surface profile of NCC-reinforced biocomposites[57,58].

4 Conclusion

Cellulose derivatives significantly affected tensile strength, elongation at break, Young's modulus, WVTR, O_2TR, WHC, swelling, glass transition temperature, crystallinity temperature, melting point, melt flow rate, and density, but did not affect the biodegradation time of the TP/GM/PLA biothermoplastic composite. The use of 2.5% NCC filler produces the best characteristics of the TP/GM/PLA biothermoplastic composite with a tensile strength value of 24,668 MPa, elongation at break of 3.123%, Young's modulus of 1.843 GPA, WVTR of 81.22 g/m^2.day, O_2TR of 85.46 ml/m^2.day, WHC of 0.17%, swelling of 2.92%, glass transition temperature of 60.98^{o}C, crystallinity temperature of 68.19^{o}C, melting point of 159.76^{o}C, melt flow rate of 8.55 g/min, density of 1.25, biodegradation time of 11.67 days, weight loss up to a temperature of 600^{o}C reaches about 12%, the highest peak of DTA is at a temperature of 493.9^{o}C with a value of about 28 µV, the peak of crystallinity occurs at an angle of 2Ɵ = 29.51^o, contains the functional group O-H (alcohol) at wave number 2952 cm^{-1}, C=O at wave number 1747 cm^{-1}, C=C (aromatic ring) at wave number 1582 cm^{-1}, C-O at wave number 1292 cm^{-1}, C=H at wave number 729 cm^{-1}, has a longitudinal surface profile with spots but their size is smaller and denser and there are no clear holes, the transverse surface profile shows that almost all the holes are closed and more compact and dense.

Acknowledgements

We would like to express our gratitude to the Research and Community Empowerment Agency (DPPM), the Ministry of Research, Technology, and Higher Education, for providing research grants and the necessary facilities to complete this research and publish this article.

Conflict of Interest

The author declares that there are no conflicts of interest with any of the authors or any other parties.

Reference

1 Kumar S, Bajaj R *et al.*:, A comprehensive review on single-use plastics (SUPs): challenges and sustainable solutions. *J of Appl Sci Innov & Tech (JASIT*), 3 (2024) 60.

2 Kumari R, Tiwari R *et al.*:, Harmful effects of plastics on human health and the environment: a review. *Int. J. of Soc. Sci. Human. Res*. 06 (2023) 248.

3 Syafaruddin M, KLHK: 80 persen sampah di laut Indonesia berasal dari aktivitas daratan, https://www.suarasurabaya.net/ekonomibisnis/2023/klhk-80-persen-sampah-di-laut-indonesia-berasal-dari-aktivitas-daratan/4, 2023, cited March 20, 2025.

4 Harsojuwono B A, Hartiati A *et al.*:, Characteristics of bio thermoplastic composite pellets based on modified cassava starch and glucomannan in variations of synthetic polymers, *Tuijin Jishu/J of Propul Tech,* 45 (2024) 1815.

5 Harsojuwono B A & Arnata I W, *Teknologi Polimer Industri Pertanian*, (Intimedia, Malang) , 2017, 75.

6 Dasan Y, Bhat A H *et al.*:, Polymer blend of PLA/PHBV based bionanocomposites reinforced with nanocrystalline cellulose for potential application as packaging material, *Carb Polym*, 157 2017 1323.

7 Douglass E F, Avci H *et al.*:, Review of cellulose and cellulose blends for preparation of bio-derived and conventional membranes, nanostructured thin films and composites, *Polym Rev,* 58 (2018), https://doi.org/10.1080/15583724.2016.1269124

8 Aranda-García F J, González-Núñez R *et al.*:, Water absorption and thermomechanical characterization of extruded starch/poly(lactic acid)/agave bagasse fiber bioplastic composites, *Int J of Polym Sci*, 1155 (2015) 343294, https://doi.org/10.1155/2015/343294

9 Ilyas R A, Sapuan S M *et al.*:, Polylactic acid (PLA) biocomposite: processing, additive manufacturing and advanced applications, *Polym (Basel),* 3 (2021) 1326. Doi: 10.3390/polym13081326

10 Ruz-Cruz M A P, Herrera-Franco J *et al.*:, Thermal and mechanical properties of PLA-based multiscale cellulosic biocomposites, *J of Mat Res and Tech*, (2022) 485, https://doi.org/10.1016/j.jmrt.2022.02.072

11 Nazrin A, Sapuan S M *et al.*:, Nanocellulose reinforced thermoplastic starch (TPS), polylactic acid (PLA) and polybutylene succinate (PBS) for food packaging applications, *Front in Chem*. (2020) 213, Doi:10.3389/fchem.2020.00213

12 Smitthipong W, Tantatherdtam R *et al.*:, Effect of pineapple leaf fiber-reinforced thermoplastic starch/poly(lactic acid) green composite: mechanical, viscosity and water resistance properties, *J of Thermoplas Comp Mat,* 28(2015) 717.

13 Alvarez V A & V´azquez A, Thermal degradation of cellulose derivatives/starch blends and sisal fibre biocomposites, *Polym Degrad and Stab,* 84 (2004) 13.

14 Campos A K, Teodoro B R *et al.*:, Properties of thermoplastic starch and TPS/polycaprolactone blend reinforced with sisal whiskers using extrusion processing, *Polym Eng & Sci*, 53 (2013) 800.

15 Ruz-Cruz M A P, Herrera-Franco J *et al.*:, Thermal and mechanical properties of PLA-based multiscale cellulosic biocomposites, *J of Mat Res and Tech*, (2022) 485. https://doi.org/10.1016/j.jmrt.2022.02.072

16 Yoksan R, Sane A *et al.*:, Effect of starch and plasticizer types and fiber content on properties of polylactic acid/thermoplastic starch blend, *Int J of Mat and Metal Eng*, 9 (2015) 1166. DOI: doi.org/10.5281/zenodo.1109605

17 Harianja B, Harsojuwono B A *et al.*:, Characteristics of biothermoplastic composites in formulation variations of thermoplastic starch, thermoplastic glucomannan and poly lactic acid, *J Rek dan Manaj Agroind*, 12 (2024) 456.

18 Saragih R N O, Harsojuwono B A *et al.*:, Characteristics of biothermoplastic composites from thermoplastic starch/thermoplastic glucomannan/polylactic acid in various types and concentrations of compatibilizer, *J Rek dan Manaj Agroind,* 12(2024) 421.

19 Harsojuwono B A, Hartiati A *et al.*:, Mechanical characteristics of biothermoplastic composite pellets made from modified cassava starch, glucomannan and polylactic acid in biofiller variations, *Tuijin Jishu/J of Propul Tech*, 46(2025) 211.

20 Kargarzadeh H, Huang J *et al.*:, Recent developments in nanocellulose-based biodegradable polymers, thermoplastic polymers, and porous nanocomposites. *Prog in Polym Sci*, 87 (2018) 197, https://doi.org/10.1016/j.progpolymsci.2018.07.008

21 Ilyas R A, Sapuan S M *et al.*:, Thermal, biodegradability and water barrier properties of bionanocomposites based on plasticised sugar palm starch and nanofibrillated celluloses from sugar palm fibres, *J. Biobased Mater Bioen*, 14 (2020) 1, doi: 10.1166/jbmb.2020.1951

22 Shojaeiarani J, Bajwa D S *et al.*:, *Cellulose Nanocrystal Based Composite*, (A Rev Comp Part C: Open Access) 5 (2021) 100164, https://doi.org/10.1016/j.jcomc.2021.100164

23 Kaya A I, Yalçın O U *et al.*:, Effects of cellulose micro and nanocrystals on the mechanical, thermal, morphological, and structural properties of rigid polyurethanes, *BioRes*, 19 (2024) 2842

24 Simangunsong D I, Hutapea T H A *et al.*:, The effect of nanocrystalline cellulose (NCC) filler on polylactic acid (PLA) nanocomposite properties, *J. Eng Techn Sci*, 50 (2018) 578.

25 Ilyas R A, Sapuan S M *et al.*:, Effect of sugar palm nanofibrillated cellulose concentrations on morphological, mechanical and physical properties of biodegradable films based on agro-waste sugar palm (*Arenga pinnata* (Wurmb.) Merr) starch. *J Mat Res Tech*, 8 (2019) 4819, doi: 10.1016/j.jmrt.2019.08.028

26 Zhang X, Tang Y *et al.*:, Dispersion and rheological properties of aqueous graphene suspensions in presence of nanocrystalline cellulose, *J of Polym and the Env*, 26 (2018) 3502, https://doi.org/10.1007/s10924-018-1237-0

27 Tomec D K, Schöflinger M *et al.*:, The effects of microcrystalline cellulose addition on the properties of wood–pla filaments for 3d printing, *Polym,* 16 (2024) 836, https://doi.org/10.3390/ polym16060836

28 Jin K, Tang Y *et al.:* , Polylactic acid based biocomposite films reinforced with silanized nanocrystalline cellulose. *Int J of Bio Macromol,* 162 (2020) 1109. https://doi.org/10.1016/j.ijbiomac.2020.06.201

29 Kusmono & Wiratma O E R. Fabrication and characterization of PLA/nanocrystalline cellulose nanocomposite filaments for 3D printing application, *Proceedings, IOP Conf Ser Mater Sci Eng,* 2021, 012055. DOI: 10.1088/1757-899X/1096/1/012055

30 Zhu J, Chen Y *et al.*:, Comprehensive insight into degradation mechanism of green biopolyester nanocomposites using functionalized cellulose nanocrystals. *ACS Sustain Chem Eng,* 7 (2019) 15537.

31 Yu H, Sun B, Reinforcement of biodegradable Poly(3-Hydroxybutyrate-Co-3-Hydroxyvalerate) with cellulose nanocrystal/silver nanohybrids as bifunctional nanofillers, *J Mater Chem B,* 2 (2014) 8479

32 Ilyas R A, Sapuan S M *et al.*:, Sugar palm nanocrystalline cellulose reinforced sugar palm starch composite: degradation and water-barrier properties, *Proceedings, IOP Conf Ser Mater Sci Eng,* 2018, 012006, doi: 10.1088/1757-899X/368/1/012006 30

33 Trifol J, Plackett D *et al.*:, A comparison of partially acetylated nanocellulose, nanocrystalline cellulose, and nanoclay as fillers for high-performance polylactide nanocomposites, *J Appl Polym Sci*, 133 (2016) 1.

34 Othman S H, Majid N A *et al.*:, Tapioca starch films reinforced with microcrystalline cellulose for potential food packaging application, *Food Sci Tech*, 39 (2019) 605, https://doi.org/10.1590/fst.36017

35 Gan P G, Sam S T *et al.*:, Thermal properties of nanocellulose-reinforced composites: A review, *J Appl Polym Sci*, 137 (2020) 48544, DOI: 10.1002/app.48544

36 Omran A A B, Mohammed A A B A *et al.*:, Micro- and nanocellulose in polymer composite materials: a review, *Polym,* 13 (2021) 231, https://doi.org/10.3390/ polym13020231

37 Khoo R Z, Ismail H *et al.*:, Thermal and Morphological properties of poly (Lactic Acid)/nanocellulose nanocomposites, *Proc. Chem*. 19 (2016) 788, doi: 10.1016/j.proche.2016.03.086

38 Spinelli G, Kotsilkova R *et al.*:, Effects of filament extrusion, 3d printing and hot-pressing on electrical and tensile properties of poly(lactic) acid composites filled with carbon nanotubes and graphene, *Nanomat*, 10 (2020) 1.

39 Bazan P, Rochman A *et al.*:, Composites based on PLA/PHBV Blends with nanocrystalline cellulose NCC: mechanical and thermal investigation, *Materials*, 17 (2024) 6036, https://doi.org/10.3390/ ma17246036 Academic

40 Chen X, Xu H *et al.*:, A Facile one-pot fabrication of polyphosphazene microsphere/carbon fiber hybrid reinforcement and its effect on the interfacial adhesion of epoxy composites, *Appl Surf Sci,* 410 (2017) 530.

41 Hu J, Chen Y *et al.*:, Comprehensive insight into degradation mechanism of green biopolyester nanocomposites using functionalized cellulose nanocrystals. *ACS Sustain Chem Eng*, 7 (2019) 15537.

42 Zhao M, Yu J *et al.*:, Facile fabrication of photochromic poly(lactic acid)/poly(3-hydroxybutyrate-co-3-hydroxyvalerate) fibers via a scalable melt-spinning process, *ACS Appl Polym Mate*r, 5 (2023) 4811.

43 Zhang K, Mohanty A K *et al.*:, Fully biodegradable and biorenewable ternary blends from polylactide, poly(3-hydroxybutyrate-co-hydroxyvalerate) and poly(butylene succinate) with balanced properties, *ACS Appl Mater Interfaces*, 4 (2012) 3091.

44 Kian L K & Jawaid M, Thermal properties of nanocrystalline cellulose and cellulose nanowhisker, *Int J Innov Technol Explor Eng*, 9 (2019) 5430.

45 Ahmad N D, Kusmono *et al.*:, Preparation and properties of cellulose nanocrystals-reinforced poly (lactic acid) composite filaments for 3d printing applications, *Results Eng*, 17 (2023) 100842.

46 Zembouai I, Bruzaud S *et al.*:, Poly(3-hydroxybutyrate-Co-3-hydroxyvalerate)/polylactide blends: thermal stability, flammability and thermo-mechanical behavior*, J Polym Environ,* 22 (2014) 131–139.

47 Phanthong P, Reubroycharoen P *et al.*:, Nanocellulose: extraction and application, *Carbon Resour Convers*, 1 (2018) 32

48 Xu Y, Wu Z *et al.:* Nanocellulose composite films in food packaging materials: a review, *Polym*, 16 (2024) 423, https://doi.org/10.3390/polym16030423

49 Arun R, Shruthy R *et al.*:, Biodegradable nano composite reinforced with cellulose nano fiber from coconut industry waste for replacing synthetic plastic food packaging, *Chemosphere*, 291 (2022) 132786

50 Raghu N, Kale A *et al.*:, Mechanical and thermal properties of wood fibers reinforced poly (lactic acid)/thermoplasticized starch composites, *J Appl Polym Sci,* 135(2018) 46118

51 Ilyas R A, Sapuan S M *et al.*:, Effect of sugar palm nanofibrillated cellulose concentrations on morphological, mechanical and physical properties of biodegradable films based on agro-waste sugar palm (*Arenga pinnata* (Wurmb.) Merr) starch, *J Mater Res Tech,* 8 (2019) 4819, doi: 10.1016/j.jmrt.2019.08.028

52 Kausar A. Green Nanocomposites for energy storage, *J Compos Sci,* 5 (2021) 202, https:// doi.org/10.3390/jcs5080202

53 Li L, Bao R Y *et al.*:, Dopamine-induced functionalization of cellulose nanocrystals with polyethylene glycol towards poly (L-lactic acid) bionanocomposites for green packaging, *Carbohydr Polym*, 203 (2019) 275.

54 Muller J, González-Martínez C *et al.*:, Poly(lactic) acid (PLA) and starch bilayer films, containing cinnamaldehyde, obtained by compression moulding, *Eur Polym J*, 95 (2017) 56.

55 Tsioptsias C, Leontiadis K *et al.*:, Experimental investigation of polypropylene composite drawn fibers with talc, wollastonite, attapulgite and single-wall carbon nanotubes, *Polym*, 4 (2022) 260, https://doi.org/10.3390/ polym14020260

56 Nazrin A, Sapuan S M *et al.*:, Flammability and physical stability of sugar palm crystalline nanocellulose reinforced thermoplastic sugar palm starch/poly(lactic acid) blend bionanocomposites, *Nanotech Rev*, 11 (2022) 86, https://doi.org/10.1515/ntrev-2022-0007

57 Chauhan S, Raghu N *et al.*:, Effect of maleic anhydride grafted polylactic acid concentration on mechanical and thermal properties of thermoplasticized starch filled polylactic acid blends, *Polym and Polym Comp,* 29 (2021) S400, https://doi.org/10.1177/09673911211004194

58 Harsojuwono B A, Arnata I W *et al.*:, The improvement of the modified starch - glucomannan - polyvinyl alcohol biothermoplastic composite characteristics with polycaprolactone and anhydride maleic acid. *Front in Sustain Food Syst,* 6 (2022) 1, doi: 10.3389/fsufs.2022.844485.